This is a peer-reviewed, accepted author manuscript of the following research article: Xie, E, Cheng, C, Ouyang, C, Hill, J, McKendry, JJD, Zhang, Y, Gu, E, Herrnsdorf, J, Haas, H & Dawson, M 2023, 'GaN-based series hybrid LED array: a dual-function light source with illumination and high-speed visible light communication capabilities', Journal of Lightwave Technology. https://doi.org/10.1109/JLT.2023.3303779

GaN-based Series Hybrid LED Array: A Dual-function Light Source with Illumination and High-speed Visible Light Communication Capabilities

Enyuan Xie, Cheng Chen, Chensui Ouyang, Jordan Hill, Jonathan J. D. McKendry, Yanchao Zhang, Erdan Gu, Johannes Herrnsdorf, Harald Haas, *Fellow, IEEE*, and Martin D. Dawson, *Fellow, IEEE*

***Abstract*—We propose and demonstrate a GaN-based series-driven hybrid light emitting diode (SH-LED) device in which broad-area and micro-LED components are interconnected for simultaneous illumination and high-speed visible light communication (VLC) applications. Through theoretical analysis based on an equivalent electrical circuit model and characterization from a fabricated exemplar device with blue emission, it is shown that SH-LEDs combine the advantages of broad-area and micro-LED components by offering high direct-current (DC) optical power output and a fast frequency response. The application of this device to VLC is demonstrated through both the point-to-point and 9° divergence-angle coverage systems at 3 m transmission distance adopting a DC-biased optical-orthogonal frequency-division multiplexing modulation scheme. Compared with a point-to-point system using a single micro-LED, that our initial demonstrator SH-LED achieves the same data transmission rate of 3.39 Gbps at forward error correction (FEC) floor of 3.8×10^{-3}, but the received DC optical power is improved by over 3 times. For the area coverage system, up to 1.56 Gbps data transmission rates at a FEC floor of 3.8×10^{-3} are accomplished by using this device, associated with over 4 times higher received DC optical power compared with that using a single micro-LED.**

***Index Terms*—Visible light communication, Series hybrid LED.**

I. Introduction

THE migration of wireless communication techniques into the unregulated visible light spectrum between 375-780 nm for data transmission is considered to be a promising approach to address the radio-frequency (RF) spectrum crunch [1]. Thanks to its inherent advantages such as improved spectral efficiency, innate security and less susceptibility to electromagnetic interference, visible light communication (VLC) technology exhibits great potential in short-distance wireless access, especially for the indoor environment [2]. Moreover, VLC technology can also be embedded into existing solid-state lighting (SSL) systems, which makes the VLC transmitters capable of being used for illumination and communication simultaneously for energy saving and novel functionality [3].

In SSL systems, GaN-based commercial blue light emitting diodes (LEDs) are commonly used which photo-excite a yellow phosphor for white light illumination. Compared with the conventional incandescent or fluorescent light sources, LEDs possess advantages such as higher power efficiency and faster modulation speed. However, due to the large resistance-capacitance (RC) time constant of the p-n junction, the modulation bandwidth of broad-area (typically 0.1-1 mm^2) LEDs (BA-LEDs), which is in the range of 10-20 MHz at -6 dB [4], is insufficient to support high-speed VLC with Gbps data rate. Therefore, different approaches such as pre-equalization, post-equalization and high-order modulation have been demonstrated to enable higher modulation bandwidth of LEDs [5]. In addition to these methods, micro-LEDs, which are with active area dimension less than 100 μm, are considered as promising light sources with high-bandwidth characteristics to enable high-speed communication. The small junction area of micro-LEDs makes these devices operating in a high current density regime with low RC effects. Consequently, modulation bandwidths of up to several hundred MHz at -6 dB can be achieved by the single micro-LEDs with different emission wavelengths covering from violet to green spectral range [6], [7], [8], [9], [10], [11]. By assuming direct current-biased optical (DCO)-orthogonal frequency division multiplexing (OFDM) modulation scheme, the data transmission rates up to 7.91 Gbps [6], 5.37 Gbps [8] and 4.65 Gbps [10] have been accomplished at the forward error correction (FEC) floor of 3.8×10^{-3} using a single micro-LED with the violet, blue and green emissions, respectively. Meanwhile, the GaN-based micro-LEDs can also be used as the photodetectors to sense short-wavelength signals and, in turn, gain the signal-to-noise ratio (SNR) in VLC systems [12], [13].

However, the small junction area of micro-LEDs results in a considerably lower light output power (LOP) than their

Enyuan Xie, Jordan Hill, Jonathan J. D. McKendry, Erdan Gu, Johannes Herrnsdorf and Martin D. Dawson are with Institute of Photonics, Department of Physics, University of Strathclyde, Glasgow, G1 1RD, U.K. (e-mail:enyuan.xie; jordan.hill; jonathan.mckendry; erdan.gu; johannes.herrnsdorf; m.dawson@strath.ac.uk).

Cheng Chen and Harald Haas are with LiFi Research and Development Centre, Department of Electronic & Electrical Engineering, University of Strathclyde, Technology & Innovation Centre, Glasgow G1 1RD, U.K. (e-mail: c.chen; harald.haas@strath.ac.uk).

Chensui Ouyang and Yanchao Zhang are with School of information science and engineering, Harbin Institute of Technology, Weihai, China (e-mail: chensui_memory@163.com; zhangyanchao66@sina.com).

Enyuan Xie and Cheng Chen contribute equally to this work.

Manuscript received April 19, 2005; revised August 26, 2015. This research was supported by Fraunhofer UK Research Ltd. and the Engineering and Physical Sciences Research Council (EP/T00097X/1). Data is available online at https://doi.org/10.15129/fecbfb1c-cc0c-4713-8f38-27ab7a1153d9. *(Corresponding auther: Yanchao Zhang and Erdan Gu)*

broad area counterparts. This issue leads not only to a limited dynamic range of optical power for communication, but also a low luminous flux r estricting t he a pplication for illumination. In order to further improve the LOP of micro-LED-based light sources, both 'in-parallel' [14], [15], [16] and 'in-series' [7], [10], [17], [18], [19] micro-LED arrays employing multiple micro-LED elements with the same size have been demonstrated for VLC applications. Compared with in-parallel micro-LED arrays, arrays with the series connection configuration h ave p referable p roperties s ince t hey produce less heat and have higher LOP, higher average external quantum efficiency (EQE) p er e lement, a nd b etter communication performance [19]. Recently, by using the series-biased micro-LED arrays and a DCO-OFDM modulation scheme, up to 9.51 Gbps [7], 6.58 Gbps [18] and 1.44 Gbps [10] data rates at the FEC floor o f 3.8×10^{-3} w ere a ccomplished at over 10 m transmission distance for violet, blue and green devices, respectively. However, with increasing the number of elements in the array for higher LOP, some potential issues raise. The increased number of elements in the array results in not only the concern about the fabrication defects potentially compromising the whole array, but also the higher demands on its driving circuit such as higher operation voltage, higher signal amplification and larger 3 dB compression point. A solution of actualizing the illumination and high-speed communication is to use high LOP BA-LEDs for illumination, and separate fast-speed micro-LEDs for VLC, each controlled by an independent driver. However, this method leads to not only non-uniform light field d istribution, b ut a lso complex design of the driving circuit and relatively high costs.

In this work, with the aim of achieving illumination and high-speed VLC applications simultaneously, a GaN-based series hybrid LED (SH-LED) device, in which the BA-LED and micro-LED components are interconnected through the series configuration, i s i ntroduced. T he e lectrical c haracteristics of this device are firstly a nalysed b ased o n a n e quivalent circuit model. Guided by this, an example device was then fabricated from a commercial blue LED wafer grown on a sapphire substrate. Both theoretical and experimental results indicate that the SH-LED possesses the characteristics of high direct-current (DC) LOP and wide bandwidth region for illumination and communication simultaneously. The higher impedance of SH-LED would also lead to an improved impedance match with the driver interface and, in turn, higher driving efficiency. The VLC applications of this SH-LED are demonstrated here in both point-to-point and area coverage systems at a 3 m center-to-center distance. In the point-to-point measurements, compared with the system using a single reference micro-LED, the one employing an SH-LED achieves the same data transmission rate of 3.39 Gbps at FEC floor o f 3.8×10^{-3}, and it can provide over 3 times higher received DC LOP. In the area coverage system measurements under a scenario relevant for the light-fidelity (LiFi) a pplication, b y u sing this SH-LED, up to 1.56 Gbps data transmission rates at FEC floor o f 3.8×10^{-3} a re a ccomplished, a ssociating w ith o ver 4 times higher received DC LOP compared with the one using a single reference micro-LED. Compared with the conventional devices, the DC LOP and frequency response characteristics of this SH-LED could be simply modified by changing the lateral dimensions of LED components following the requirements at different application scenarios. Furthermore, the SH-LEDs with a limited number of LED components have the advantages of the high fabrication yield, simple addressing method and moderate driving requirement. These make this novel device approach a promising light source with both illumination and communication capabilities.

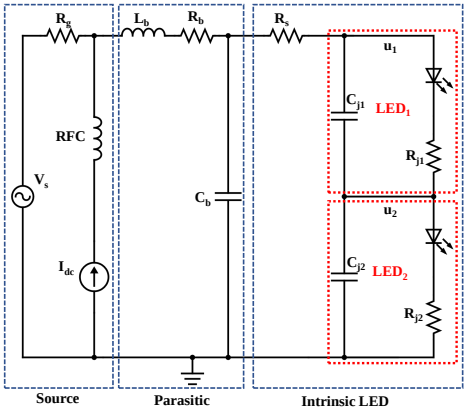

Fig. 1. Equivalent circuit model of an SH-LED.

II. Theoretical Analysis on the Electrical Characteristics of Series Hybrid LEDs

With the purpose of investigating the electrical characteristics of SH-LEDs, the equivalent circuit of an SH-LED driven by the alternating-current (AC) signal source at an offset DC current is developed. As shown in Fig.1, this model comprises a source, parasitic, and intrinsic LED parts. The source part comprises the DC constant current power supply I_{dc}, choke RFC, AC signal source V_s and electrical impedance R_g. The parasitic parameters contributed from wire-leads and cable connections include parasitic inductance L_b, parasitic resistance R_b and parasitic capacitance C_b. The intrinsic LED part represents the SH-LEDs developed in this work, in which two LEDs are series connected. Since ideal diode models are employed in the circuit, the equivalent capacitance of p-n junction C_{jn} and resistance R_{jn} are introduced to differentiate two LEDs with different p-n junction area. R_s in the circuit is the series resistance from the metal tracks in the SH-LED.

Based on the circuit shown in Fig.1, the equivalent impedance of SH-LED, Z_{SH-LED}, is expressed as:

$$Z_{SH-LED} = \left[R_s + (R_{j1} // \frac{1}{j\omega C_{j1}}) + (R_{j2} // \frac{1}{j\omega C_{j2}})\right] // \frac{1}{j\omega C_b} + R_b + j\omega L_b \quad (1)$$

where ω is the angular frequency of the AC signals. It is well known that a single LED normally possesses a low impedance with capacitive characteristics. Thus, there is a significant impedance mismatch between conventional RF drivers with 50 impedance and a single LED, which leads to a low driving efficiency. From (1), it can be found that, thanks to the employed series connection configuration, a lower parasitic capacitance

and higher impedance can be achieved for SH-LEDs. This characteristic would lead to an improved impedance mismatch and, thus, higher driving efficiency for SH-LEDs.

The AC voltages dropped on the different LED components in SH-LED, u_1 and u_2 in Fig.1, can be further expressed as:

$$u_1 = \frac{R_{j1} + j\omega R_{j1}R_{j2}C_{j2}}{\alpha} u_s, \tag{2}$$

$$u_2 = \frac{R_{j2} + j\omega R_{j1}R_{j2}C_{j1}}{\alpha} u_s, \tag{3}$$

$$\begin{aligned}\alpha =& (R_g + R_b + j\omega L_b)(1 + j\omega R_{j1}C_{j1})(1 + j\omega R_{j2}C_{j2}) \\ &+ (R_{j1} + R_{j2} + j\omega R_{j1}R_{j2}C_{j1} + j\omega R_{j1}R_{j2}C_{j2}) \\ &\left[1 + j\omega C_b(R_g + R_b) - \omega^2 C_b L_b\right],\end{aligned} \tag{4}$$

where u_s is the AC voltage supplied from AC signal source V_s. Based on (2) and (3), it is clear that the AC voltage dropped on a certain LED component depends on its own resistance and the capacitance from another LED component in the circuit. Assuming the LED_1 and LED_2 represent the BA-LED and micro-LED components, lower R_{j1}, higher R_{j2}, larger C_{j1} and smaller C_{j2} are expected. Thus, the AC driving signal dropped on the micro-LED component would always be greater than the one on the BA-LED component. Furthermore, as ω increases, the u_1 attenuates quickly in the low frequency regions and, consequently, nearly all AC driving signals are applied on the micro-LED component in the high frequency regions. These analyses indicate that, although the BA-LED component leads to a fast decay with frequency response in the low frequency regions, the micro-LED component plays a dominant role in determining the bandwidth range of SH-LED used for data transmission. Here it is also important to point out that, since the DC current going through both LED components of the SH-LEDs are the same (I_{dc} in Fig.1), the DC LOP is dominated by the BA-LED component. Thus, the SH-LED possesses both advantages of BA-LED and micro-LED of high DC LOP and wide modulation frequency range simultaneously.

III. Design and Fabrication of Series Hybrid LEDs

A demonstration implementation of the SH-LED concept in a flip-chip configuration was fabricated from commercial blue (nominal λ = 450 nm) GaN-based LED wafers grown on 2 inch c-plane (0001) sapphire with periodically patterned surfaces. The detailed epitaxial structure of the wafers can be found in [20]. The fabrication process of this device is similar to the one we developed for fabricating series-biased micro-LED arrays, which has been described in detail in [17]. In this fabrication process, a dual-plasma etching step is introduced to define the different-size LED components and isolate each component from both p- and n-type GaN. An optimized Pd-based metal layer is utilized as the p-type ohmic contact and reflector to ensure the excellent electrical and optical performance. The risk of forming short-circuits in the series connection configuration is addressed by employing a plasma ashing step. Fig.2(a) shows a plan-view optical image of the as-fabricated SH-LED device. As shown, in order to achieve a homogeneous light-field distribution, a concentric design is

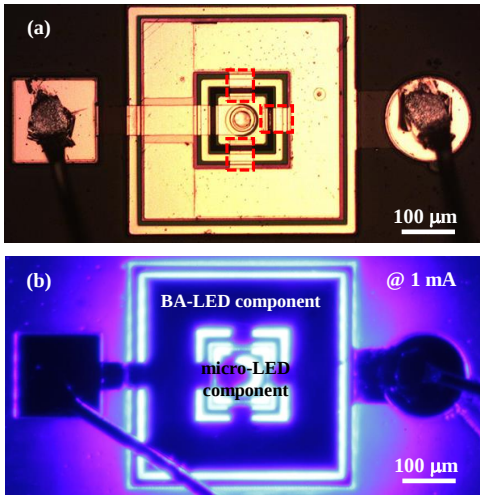

Fig. 2. Plan-view optical images of (a) as-fabricated SH-LED and (b) operating device at a DC current of 1 mA. The multiple series-interconnecting metal tracks are highlighted by the red dash rectangles in (a).

employed for this example device, in which a 40 μm-diameter central micro-LED component is surrounded by a homocentric square shaped BA-LED component with a 10 μm gap between the micro-LED and BA-LED components. The emission area of the BA-LED component is equivalent to a square-shaped LED with 300 μm side lengths. The chosen sizes of micro-LED and BA-LED components reflect the typical dimensions used in our previous work representing micro-scale and normal LEDs, which could be modified to permit different application requirements as discussed in section IV. Meanwhile, in this device design, multiple series-interconnecting metal tracks highlighted by the red dash rectangles in the figure have been introduced between the LED components to guarantee a uniform current spreading, especially for the BA-LED component. Fig.2(b) shows an optical image of the fabricated SH-LEDs operating at a DC current of 1 mA. With the purpose of performance comparison, stand-alone individually-addressable reference micro-LEDs with a diameter of 40 μm are fabricated as well. The devices are then wire-bonded to a printed circuit board (without a heatsink installed) for further characterizations and VLC measurements.

IV. Electrical, Optical and Frequency Response Characterizations of Series Hybrid LEDs

Fig.3(a) presents the current versus voltage (I-V) and LOP versus current (L-I) characteristics of the fabricated SH-LED and micro-LED, respectively. By placing a Si photodetector in close proximity to the polished sapphire substrate, these characteristics were measured at the same time through scanning each current point under DC conditions. As shown, due to the introduced BA-LED component in the SH-LED, the turn-on voltage at 1 mA operation current of this device increases from 3.1 V to 5.6 V compared with the one of a single micro-LED. Meanwhile, a series-resistance around 23.3 Ω is extracted for SH-LED, which is about 4.3 Ω higher than the one from a single micro-LED. Although the BA-LED component in the SH-LED devices introduces the additional operation voltage

and series-resistance, no noticeable differences in the current handling capabilities are observed between the SH-LED and single micro-LED. This phenomenon guarantees the high operation current densities applied to the micro-LED component and, in-turn, promising communication performance. When comparing LOP, the SH-LED produces over 4 times higher LOP than the single micro-LED. Before thermal roll-over, LOP around 13.0 mW and 2.8 mW are achieved by SH-LED and micro-LED, respectively. It is important to highlight that the improvements on the LOP of the SH-LED strongly depends on the size of its BA-LED component, which offers flexibility in design targeted at applications with different requirements on the LOP. This enhanced LOP contributed from the BA-LED component further results in an improvement of the EQE of SH-LED. As shown in Fig.3(b), the peak EQE of the SH-LED is abut 25.6% at 1 mA, which is about 2 times higher than the peak value of the micro-LED of 12.6% at 0.3 mA. Furthermore, the EQE droop behaviors are also reduced from 73.9% in the micro-LED to 40.2% in the SH-LED at the operation current of 85 mA. Similar phenomena are observed for the wall plug efficiency (WPE) shown in Fig.3(c). Although the additional operation voltage and series-resistance lead to a similar peak WPE between SH-LED and micro-LED, the SH-LED presents lower efficiency droop of 64.1% compared with 87.5% from the micro-LED at the operation current of 85 mA. These mitigations on the efficiency droop may be attributed to the employed BA-LED component and series-connection configuration in the SH-LED [21]. Here, we also wish to emphasize that, as the micro-LED component in the SH-LED device can only sustain a lower current, the operation current region of the SH-LED is strongly restricted. This results in a limitation on the maximum LOP achieved by the SH-LED. We are currently developing a new methodology to overcome this issue. Fig.3(d) illustrates the normalized irradiance beam profiles of the fabricated devices measured at an operation current of 50 mA and 0.1 m distance between the devices and a Si photodetector. There is no significant difference in the angular dependence of the emitted light between the devices. The near Lambertian irradiation intensity distributions with viewing half angles of 57° and 52° are observed for SH-LED and micro-LED, respectively. The slightly wider viewing half angle of SH-LED can be attributed to its BA-LED component and is consistent with the results reported in [22].

As demonstrated in section II, the frequency responses of the SH-LED are dominated by different-size components in different frequency regions. Thus, as shown as the inset of Fig.4, the conventional single bandwidth value at certain decibel level, such as -6 dB in [8], is no longer suitable to be used for the performance comparison between SH-LED and micro-LED. Here, we employed the channel gain of frequency-selective fading $|H(f)|^2$ to evaluate the frequency response of SH-LED and micro-LED. The experimental setup of the measurements is similar to the one we used in [18]. The 4-quadrature amplitude modulation (QAM) waveforms generated by MATLAB® were forwarded to an arbitrary waveform generator (AWG, Keysight M8195A). The output analog signals from AWG were firstly amplified by a high-power amplifier (SHF S126A) and then applied to the LED devices combined with the DC current through a bias-T (Tektronix PSPL5575A). The optimized modulation signal depths from AWG, V_{PP}, were set as 0.42 V and 0.34 V for SH-LED and micro-LED, respectively. The light emitted from the devices was firstly collimated by the Tx optics (Edmund

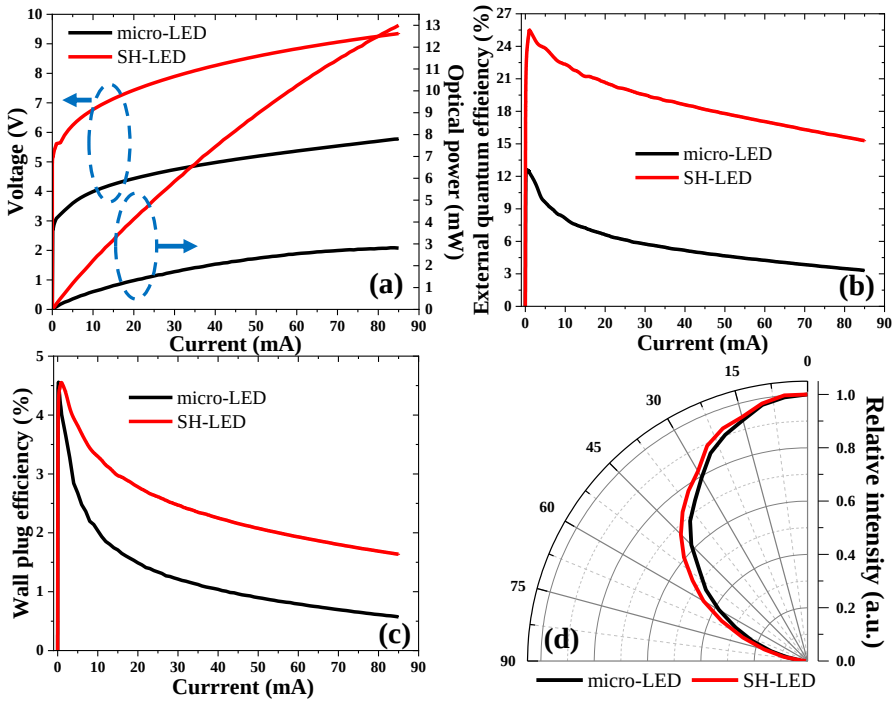

Fig. 3. (a) I-V, L-I, (b) EQE and (c) WPE of the fabricated SH-LED and micro-LED; (d) Normalized irradiance beam profiles of the fabricated SH-LED andmicro-LED measured at 50 mA and a distance of 0.1 m.

Optics 15542) and focused onto a fast-speed photoreceiver (Femto HSPR-X-I-1G4-SI) by the Rx optics (Edmund Optics 15542) with a 0.2 m transmission distance. The output signals of the photodetector were captured by a digital oscilloscope (Keysight MXR608A) and sent back to the PC. The channel gains as a function of frequency of the devices were further determined by the ratios between the detected symbols and the original pilot symbols. Fig.4 illustrates the typical channel gains achieved for SH-LED and micro-LED at a DC operation current of 50 mA. As shown, the micro-LED presnets a slow decay over the measured frequency region demonstrating its fast-modualtion-speed characteristic. On the other hand, the channel gain of the SH-LED is dominated by its different-size components in different frequency regions, which drops significantly i n t he fi rst 10 0 MH z re gion an d th en follows a slower decay similar to that of the micro-LED. This phenomenon demonstrates not only that the SH-LED benefits from a wide bandwidth region contributed from its micro-LED component to facilitate high-speed communications, but also the minimal effect of rapid attenuation from BA-LED component on the frequency response characteristic of micro-LED component. Furthermore, compared with the micro-LED, the SH-LED presents a higher channel gain especially in the low frequency region. This enhancement should be mainly attributed to the additional strength of optical channel from the BA-LED component in the SH-LED. In the meantime, as discussed in section II, the AC voltage dropped on the micro-LED component increases with signal frequency increasing. It would also lead to a higher strength of optical channel from the micro-LED component and, in turn, higher channel gain.

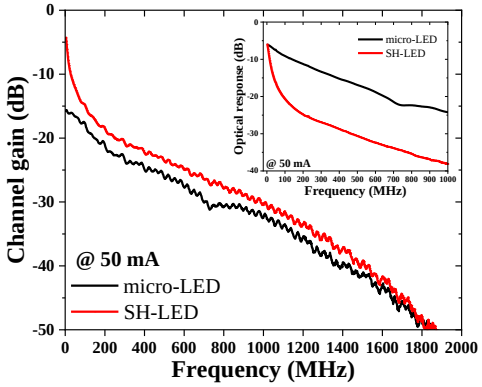

Fig. 4. Typical channel gains achieved by the fabricated SH-LED and micro-LED. The inset shows the measured optical responses for the same LEDs using vector network analyzer.

V. VLC APPLICATIONS OF SERIES HYBRID LED IN POINT-TO-POINT AND COVERAGE SYSTEMS

In this section, the performance of a free-space VLC system employing an SH-LED as transmitter is presented where DCO-OFDM is used in conjunction with an adaptive bit and energy loading algorithm [6], [23]. In addition to the results from the conventional point-to-point communication system, results from the system with defined coverage area are also demonstrated. The achieved data transmission rate and received DC LOP are further compared with those measured from the same system using a single reference micro-LED as a transmitter. Fig.5 shows a block diagram of the setup used in this work for free-space VLC systems with DCO-OFDM, which is similar to that described in section IV for channel gain measurements. By changing the objective distance between the LEDs and Tx optics, the divergence angle of the light source could be adjusted and, in turn, the communication system could be converted from point-to-point to area coverage. The data transmission distance in the following point-to-point system is set as 3 m and a wideband PIN photodiode (Femto HSPR-X-I-1G4-SI) is used as the receiver. For the coverage system, the divergence angle of the light source is set at around 9° corresponding to a 50 cm diameter coverage area at 3 m center-to-center distance. To enhance the detected signal strength, an avalanche photodiode (Hamamatsu C5658) is employed as the receiver. The DC operation current is limited as 50 mA for both SH-LED and micro-LED in the measurements to avoid the influence of heating effects. The detailed information of the DCO-OFDM scheme used can be found in [6], [23].

A. Point-to-point VLC system

The SNR versus frequency from the point-to-point system using SH-LED and micro-LED with DCO-OFDM modulation format are shown in Fig.6(a). The optimized V_{PP} from the AWG used for SH-LED and micro-LED are 0.47 V and 0.36 V, respectively. As shown, due to the contribution from the micro-LED component in the SH-LED, the SNR curves achieved by both LEDs present similar frequency coverage. Up to 1.5 GHz bandwidth is accomplished with and SNR value higher than 0 dB. Such a wide frequency region allows substantial numbers of parallel channels for bit loading in the DCO-OFDM format to approach the limitation of data capacity. However, a significant difference in the SNR performances between the SH-LED and micro-LED can be observed in the first 100 MHz as highlighted in the inset of Fig.6(a). The SNR values of SH-LED are limited at around 17.0 dB at very low frequencies and increase sharply to similar values to the micro-LED when the frequency is over 40 MHz. It is well-known that, in VLC systems, the achievable SNR value of each subcarrier is limited by both receiver noise and nonlinear distortion. In order to further investigate the mechanisms of the observed SNR degradation of the SH-LED in the low frequency region, an approach estimating the SNR values solely deteriorated by receiver noise is introduced [24]. In this approach, identical training symbols are used on each subcarrier across all OFDM frames. The resultant estimating SNR curves achieved by SH-LED and micro-LED are shown in Fig.6(b). Due to its higher channel gain as discussed in section IV, compared with the micro-LED, the SH-LED achieves higher SNR values under the sole effect of receiver noise especially in the low frequency region, which is contrary to the SNR performance under the effects of both receiver noise and nonlinear distortion. Thus, the nonlinear distortions from the BA-LED component in the SH-LED are considered as the main factor leading to the observed SNR degradation in the low frequency region shown in Fig.6(a). It has been reported in [25] that the nonlinear

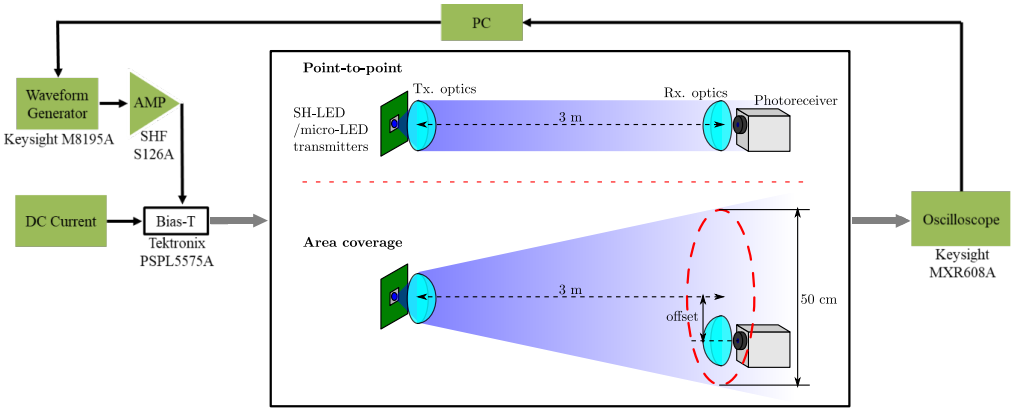

Fig. 5. Schematic block diagram of the setup used for point-to-point and area coverage VLC measurements.

distortion resulting from the voltage-optical power behavior of LEDs strongly depends on the chip size, which is well consistent with the results observed in this work.

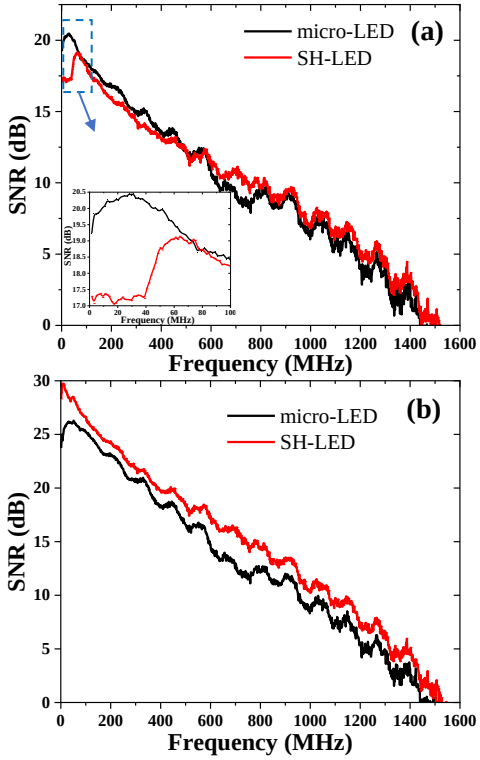

Fig. 6. (a) SNR versus frequency for the free-space point-to-point VLC systems using SH-LED and micro-LED with a 3 m data transmission distance, the inset shows the detailed SNR performance in the first 100 MHz; (b) SNR under the sole effect of receiver noise versus frequency for the same VLC systems shown in part (a).

Fig.7 illustrates the measured data transmission rates against bit error rate (BER) for the VLC systems using SH-LED and micro-LED, respectively. As shown, although the SH-LED presents slightly worse SNR performance in the low frequency region, the achieved data transmission rates are generally identical for VLC systems using different LEDs due to the similar frequency characteristics and optical-power dynamic region contributed from the micro-LED. Up to 3.39 Gbps data transmission rate is accomplished at the forward error correction (FEC) floor of 3.8×10^{-3} for both systems. Meanwhile, the received DC LOP at the receiver part after lens focusing is measured as 1.30 mW for the system using SH-LED, which is over 3 times higher than the one measured for the system using the micro-LED. These results are well consistent with the analyses in section II indicating that the system with SH-LED fully exploits the advantages from its BA-LED component on the DC LOP and micro-LED component on the frequency response, respectively. This characteristic makes this innovative device a promising candidate as the light source for systems requiring both high DC optical power illumination and high-speed communications, such as light-fidelity (LiFi) applications.

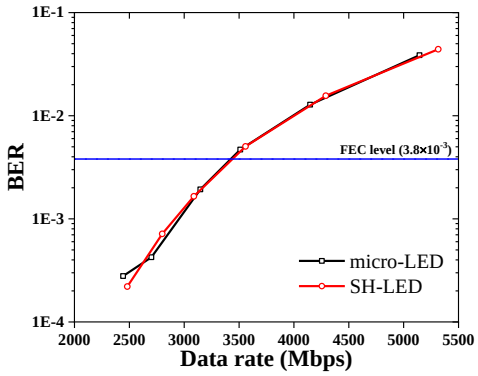

Fig. 7. Measured data transmission rates against BER for the free-space point-to-point VLC systems using SH-LED and micro-LED with a 3 m data transmission distance.

B. Area coverage VLC system

As described above, a VLC system covering an illumination region with a 50 cm diameter at 3 m center-to-center distance has been implemented to characterise the performance of different LEDs under a scenario highly relevant for LiFi applications. Fig.8(a) summarises the achieved data rates at FEC floor of 3.8×10^{-3} at different offsets (the distance between the measurement point and the center of the illuminated region) for the area coverage VLC systems using SH-LED and micro-LED, respectively. In order to avoid the influence of stray light,

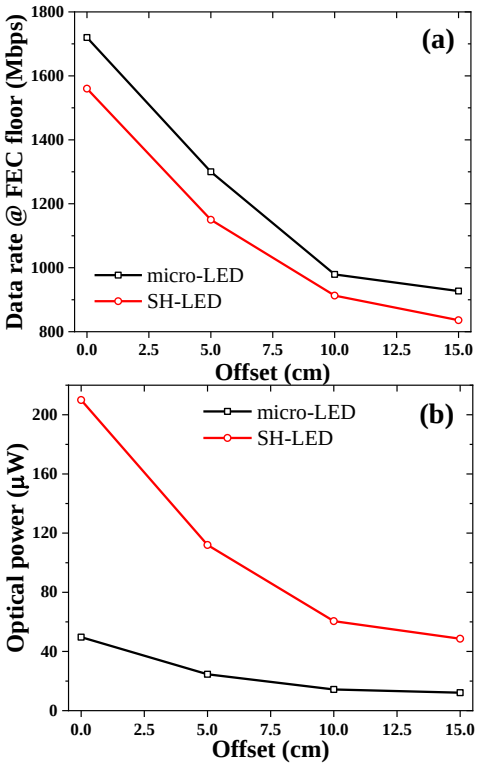

Fig. 8. Measured (a) data transmission rates at the FEC floor of 3.8×10^{-3} and (b) DC LOP at different offsets for the free-space area coverage VLC systems using SH-LED and micro-LED, respectively, with a 9° divergence angle and 3 m center-to-center distance.

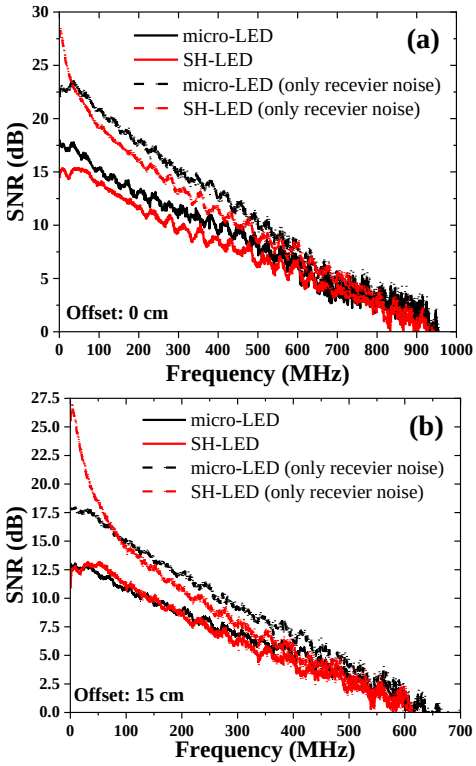

Fig. 9. SNR versus frequency for the free-space area coverage VLC systems using SH-LED and micro-LED at the offsets of (a) 0 cm and (b) 15 cm. The dash curves in each part represent the SNRs estimated under the sole effect of receiver noises for different LEDs at the same offset.

the corresponding lateral offsets for the data shown here are limited to 15 cm though the actual radius of the coverage area is 25 cm. Thanks to the concentric design employed for the SH-LED, the achieved data rates at the FEC floor of 3.8×10^{-3} for both systems follow the same trend in lower data rates at larger offsets. As shown in Fig.8(b), the irradiance intensities of both systems follow a Gaussian distribution, which results in a lower DC LOP received at larger offsets and, in turn, lower data rates. For the system using SH-LED, up to 1.56, 1.15, 0.91, and 0.84 Gbps data rates, respectively, are accomplished at offsets of 0, 5, 10, and 15 cm. These values are around 9% lower compared with the ones achieved by the system using the micro-LED at the same offsets. When comparing DC LOP, the system using the SH-LED presents about 4 times higher values than the one using the micro-LED at the same offsets. These results confirm the innovative characteristics of SH-LED with high DC LOP and wider frequency region utility contributed from its different-size components. Meanwhile, the promising illumination and communication performance achieved by the area coverage system using the SH-LED further demonstrates the great potential of SH-LED for LiFi applications. As discussed in section IV, we are carrying out optimization works on the device design, including LED component size selection and configuration modification, to further improve the device performance on both illumination and communication applications.

In order to investigate the differences in the data transmission rates achieved by SH-LED and micro-LED in area coverage VLC systems, the SNR curves of both LEDs at the offsets of 0 and 15 cm are shown in Fig.9(a) and (b), respectively. The corresponding SNR curves under the sole effect of receiver noise are also included in the figures as dashed plots for comparison purposes. As shown, at both offsets, the observed differences in the low frequency region between the SNR curves under different estimations are similar to the results shown in Fig.6. Thus, we could attribute the degraded SNR performance of the SH-LED in the low frequency region to the severe nonlinear distortions from its BA-LED component. On the other hand, compared with the micro-LED, the SH-LED presents lower SNR values at higher frequencies under both estimations. The relatively small modulation signal power applied on the SH-LED, which is mainly limited by the high-power amplifier used in this work, is considered as the main factor leading to this phenomenon. In our previous work, it has been demonstrated that the SNR performance at high frequencies can be significantly improved by the large signal swing thanks to the increased modulation signal power [6]. Due to the high path loss in the coverage VLC measurements, a large modulation signal power should be used for obtaining the optimized SNR performance and, in turn, highest data transmission rates, especially for the SH-LED employing series-connection configurations. However, the 3 dB compression point of the used amplifier limits the maximum modulation signal power applied on SH-LED. It has been found in our experiments that further increases in the V_{PP} from AWG for SH-LED do not lead to the improvements

in the achieved SNR. This results in a considerable small modulation signal power and, in turn, lower SNR values at high frequencies for the SH-LED. It is expected that the higher data transmission rates for the system using an SH-LED, which are similar to those achieved by the system using a micro-LED, should be accomplished when a high-performance amplifier i s employed.

VI. Conclusion

In this work, we propose an innovative GaN-based SH-LED concept, which employs a series configuration to interconnect the conventional BA-LED and micro-LED components together in a single chip, as a promising light source for high-speed VLC systems with illumination capabilities. Compared with the conventional LED devices, this SH-LED offers several advantages such as flexible design strategy, high fabrication yield, simple addressing method and moderate driving requirement. The performance of this SH-LED was investigated through the theoretical analysis based on an equivalent electrical circuit and experimental characterization from a fabricated example demonstrator device with blue emission. The results indicate that, thanks to the contributions from its different-size components, the SH-LED possesses the combined benefits of high DC LOP for illumination and wide modulation bandwidth for communications. In order to demonstrate its applications in VLC, this SH-LED is further employed as a transmitter in point-to-point and area coverage demonstrator communication systems with a 3 m center-to-center distance. Compared with the systems using a reference micro-LED, those using the SH-LED achieve not only similar data transmission rates but also higher DC LOP. Utilizing a DCO-OFDM modulation format, up to 3.39 and 1.56 Gbps respective data transmission rates at a FEC floor of 3.8×10^{-3} are accomplished by the SH-LED in point-to-point and area coverage VLC systems, associated with over 3 and 4 times higher received DC LOP, respectively, compared with the systems using a micro-LED. Further improvements are expected by optimizing this design.

References

[1] H. Burchardt, N. Serafimovski, D. Tsonev, S. Videv, and H. Haas, "VLC: Beyond point-to-point communication," *IEEE Communications Magazine*, vol. 52, no. 7, pp. 98–105, 2014.

[2] H. Elgala, R. Mesleh, and H. Haas, "Indoor optical wireless communication: potential and state-of-the-art," *IEEE Communications Magazine*, vol. 49, no. 9, pp. 56–62, 2011.

[3] H. Haas, L. Yin, Y. Wang, and C. Chen, "What is lifi?" *Journal of lightwave technology*, vol. 34, no. 6, pp. 1533–1544, 2015.

[4] J. Grubor, S. C. J. Lee, K.-D. Langer, T. Koonen, and J. W. Walewski, "Wireless high-speed data transmission with phosphorescent white-light LEDs," in *33rd European Conference and Exhibition of Optical Communication-Post-Deadline Papers (published 2008)*. VDE, 2007, pp. 1–2.

[5] X. Huang, J. Shi, J. Li, Y. Wang, and N. Chi, "A Gb/s VLC transmission using hardware preequalization circuit," *IEEE photonics technology letters*, vol. 27, no. 18, pp. 1915–1918, 2015.

[6] M. S. Islim, R. X. Ferreira, X. He, E. Xie, S. Videv, S. Viola, S. Watson, N. Bamiedakis, R. V. Penty, I. H. White *et al.*, "Towards 10 Gb/s orthogonal frequency division multiplexing-based visible light communication using a GaN violet micro-LED," *Photonics Research*, vol. 5, no. 2, pp. A35–A43, 2017.

[7] Z. Jin, L. Yan, S. Zhu, X. Cui, and P. Tian, "10-Gbps visible light communication in a 10-m free space based on violet series-biased micro-LED array and distance adaptive pre-equalization," *Optics Letters*, vol. 48, no. 8, pp. 2026–2029, 2023.

[8] R. X. Ferreira, E. Xie, J. J. McKendry, S. Rajbhandari, H. Chun, G. Faulkner, S. Watson, A. E. Kelly, E. Gu, R. V. Penty *et al.*, "High bandwidth GaN-based micro-LEDs for multi-Gb/s visible light communications," *IEEE Photonics Technology Letters*, vol. 28, no. 19, pp. 2023–2026, 2016.

[9] Z. Zhu, L. Lei, T. Lin, L. Li, Z. Lin, H. Jiang, G. Li, and W. Wang, "Embedded Electrode Micro-LEDs With High Modulation Bandwidth for Visible Light Communication," *IEEE Transactions on Electron Devices*, 2022.

[10] S. Zhu, X. Shan, R. Lin, P. Qiu, Z. Wang, X. Lu, L. Yan, X. Cui, G. Zhang, and P. Tian, "Characteristics of GaN-on-Si Green Micro-LED for Wide Color Gamut Display and High-Speed Visible Light Communication," *ACS Photonics*, 2022.

[11] G. Li, R. Lin, H. Guo, P. Tian, and N. Chi, "Visible light communication system at 3.59 Gbit/s based on c-plane green micro-LED," *Chinese Optics Letters*, vol. 20, no. 11, p. 110602, 2022.

[12] R. Lin, X. Liu, G. Zhou, Z. Qian, X. Cui, and P. Tian, "InGaN micro-LED array enabled advanced underwater wireless optical communication and underwater charging," *Advanced optical materials*, vol. 9, no. 12, p. 2002211, 2021.

[13] J. Shi, Z. Xu, W. Niu, D. Li, X. Wu, Z. Li, J. Zhang, C. Shen, G. Wang, X. Wang *et al.*, "Si-substrate vertical-structure InGaN/GaN micro-LED-based photodetector for beyond 10 Gbps visible light communication," *Photonics Research*, vol. 10, no. 10, pp. 2394–2404, 2022.

[14] S. Yao, H. Chai, L. Lei, Z. Zhu, G. Li, and W. Wang, "Parallel micro-LED arrays with a high modulation bandwidth for a visible light communication," *Optics Letters*, vol. 47, no. 14, pp. 3584–3587, 2022.

[15] H. Chai, S. Yao, L. Lei, Z. Zhu, G. Li, and W. Wang, "High-Speed Parallel Micro-LED Arrays on Si Substrates Based on Via-Holes Structure for Visible Light Communication," *IEEE Electron Device Letters*, vol. 43, no. 8, pp. 1279–1282, 2022.

[16] Z. Wei, M. Li, Z. Liu, Z. Wang, C. Zhang, C.-J. Chen, M.-C. Wu, Y. Yang, C. Yu, and H. Fu, "Parallel mini/micro-LEDs transmitter: Size-dependent effect and Gbps multi-user visible light communication," *Journal of Lightwave Technology*, vol. 40, no. 8, pp. 2329–2340, 2021.

[17] E. Xie, X. He, M. S. Islim, A. A. Purwita, J. J. McKendry, E. Gu, H. Haas, and M. D. Dawson, "High-speed visible light communication based on a III-nitride series-biased micro-LED array," *Journal of Lightwave Technology*, vol. 37, no. 4, pp. 1180–1186, 2018.

[18] E. Xie, R. Bian, X. He, M. S. Islim, C. Chen, J. J. McKendry, E. Gu, H. Haas, and M. D. Dawson, "Over 10 Gbps VLC for long-distance applications using a GaN-based series-biased micro-LED array," *IEEE Photonics Technology Letters*, vol. 32, no. 9, pp. 499–502, 2020.

[19] H. Huang, H. Wu, C. Huang, T. Lan, Q. Han, S. Zheng, and H. Wang, "Cascade GaN-based blue micro-light-emitting diodes for dual function of illumination and visible light communication," *Journal of Physics D: Applied Physics*, vol. 53, no. 35, p. 355103, 2020.

[20] E. Xie, M. Stonehouse, R. Ferreira, J. J. McKendry, J. Herrnsdorf, X. He, S. Rajbhandari, H. Chun, A. V. Jalajakumari, O. Almer *et al.*, "Design, fabrication, and application of GaN-based micro-LED arrays with individual addressing by N-electrodes," *IEEE Photonics Journal*, vol. 9, no. 6, pp. 1–11, 2017.

[21] C. Wang, D. Lin, C. Lee, M. Tsai, G. Chen, H. Kuo, W. Hsu, H.-C. Kuo, T. Lu, S. Wang *et al.*, "Efficiency and droop improvement in GaN-based high-voltage light-emitting diodes," *IEEE Electron Device Letters*, vol. 32, no. 8, pp. 1098–1100, 2011.

[22] H. Choi, M. Dawson, P. Edwards, and R. Martin, "High extraction efficiency InGaN micro-ring light-emitting diodes," *Applied physics letters*, vol. 83, no. 22, pp. 4483–4485, 2003.

[23] D. Tsonev, H. Chun, S. Rajbhandari, J. J. McKendry, S. Videv, E. Gu, M. Haji, S. Watson, A. E. Kelly, G. Faulkner *et al.*, "A 3-Gb/s Single-LED OFDM-Based Wireless VLC Link Using a Gallium Nitride μLED," *IEEE photonics technology letters*, vol. 26, no. 7, pp. 637–640, 2014.

[24] D. A. Tsonev, "High speed energy efficient incoherent optical wireless communications," Ph.D. dissertation, University of Edinburgh, 2015.

[25] Z. Sun, D. Teng, L. Liu, X. Huang, X. Zhang, K. Sun, Y. Wang, N. Chi, and G. Wang, "A power-type single GaN-based blue LED with improved linearity for 3 Gb/s free-space VLC without pre-equalization," *IEEE Photonics Journal*, vol. 8, no. 3, pp. 1–8, 2016.